Stress Relaxation via Addition−Fragmentation Chain Transfer in a Thiol-ene Photopolymerization

Christopher J. Kloxin, Timothy F. Scott,† and Christopher N. Bowman*

Department of Chemical and Biological Engineering, University of Colorado, Boulder, Colorado 80309-0424

Received December 11, 2008; Revised Manuscript Received February 3, 2009

ABSTRACT: Allyl sulfide addition−fragmentation chain transfer was employed concurrently with the radical-mediated formation of a thiol-ene network to enable network adaptation and mitigation of polymerization-induced shrinkage stress. This result represents the first demonstration of simultaneous polymerization and network adaptation in covalently cross-linked networks with significant implications for the fabrication of low-stress polymer networks. For comparison, analogous networks incorporating propyl sulfide moieties, incapable of addition−fragmentation, were synthesized and evaluated in parallel. At the highest irradiation intensity, the allyl sulfide-containing material demonstrated a >75% reduction in the final stress when compared with the propyl sulfide-containing material. Analysis of the conversion evolution revealed that allyl sulfide addition−fragmentation decreased the polymerization rate owing to thiyl radical sequestration. Slow consumption of the allyl sulfide functional group suggests that intramolecular hydrolytic substitution occurs by a stepwise, rather than concerted, mechanism. Simultaneous stress and conversion measurements demonstrated that the initial stress evolution was identical for both the allyl and propyl sulfide-containing materials but diverged after gelation. Whereas addition−fragmentation chain transfer was found to occur throughout the polymerization, its effect on the stress evolution was concentrated toward the end of polymerization when network rearrangement becomes the dominant mechanism for stress relaxation. Even after the polymerization reaction was completed, the polymerization-induced shrinkage stress in the allyl sulfide-containing material continued to decrease, exhibiting a maximum in the stress evolution and demonstrating the potential for continuing, longer-term stress relaxation.

Introduction

Rapid conversion of vinyl monomers to polymer, which is common in photopolymerization reactions,[1] is typically accompanied by significant volume shrinkage, effecting shrinkage stress that is frequently detrimental to both mechanical and optical material properties in applications including coatings,[2] adhesives,[3] lenses,[4,5] and dental materials.[6−8] In principle, polymerization-induced shrinkage stress is dissipated by viscous flow preceding gelation and accumulates after the formation of an incipient gel. When the reaction reaches final conversion, the stress becomes irreversibly set by the network structure.

There are several strategies for combating the deleterious effects of shrinkage stress in rapid free-radical polymerizations. One common mitigation approach is the minimization of polymerization shrinkage, which is achievable through a variety of means. Oligomeric polymerizable species have been used to reduce polymerization shrinkage and subsequent shrinkage because the concentration of reactive species is low.[9] Additionally, ring-opening polymerizations, such as those employing epoxy[10] or spiro[11] compounds and polymerization-induced microphase separation[12,13] have shown great potential to reduce volume shrinkage. However, upon full conversion to a chemical gel, there are very few mechanisms to alleviate shrinkage stress without effecting irreversible network degradation.

In previous work, post-polymerization stress relief was demonstrated by the introduction of radical species to a network containing allyl sulfide functionalities.[14] Allyl sulfide addition−fragmentation (i.e., intramolecular homolytic substitution, S_H2')[15,16] has been utilized in a variety of synthetic schemes,[17,18] including methods for synthesizing low-polydispersity linear polymers.[19−21] Incorporation of the allyl sulfide functionality into a chemical network allows for bond rearrangement via addition−fragmentation chain transfer. This reaction preserves the concentration of both the allyl sulfide and thiyl radical reactants, which subsequently participate in further addition−fragmentation events. (See Scheme 1.) This addition−fragmentation reaction cascade, where an active center effectively diffuses throughout the network, enables a global reduction in stress without concomitant network degradation.

Radical-mediated photopolymerizations of mercaptan and electron-rich vinyl monomers (i.e, thiol-ene photopolymerizations) have received much attention owing to their low shrinkage stress relative to the commonly utilized (meth)acrylate chain-growth photopolymerizations. Thiol-ene polymerizations proceed via a step-growth mechanism, whereby propagation and chain transfer reactions alternate (Scheme 2).[22,23] This mechanism results in geometric molecular weight growth, which significantly delays the gel-point conversion when compared with that of typical chain-growth free-radical mechanisms.[24,25]

Here allyl sulfide addition−fragmentation is demonstrated to bring about stress relief during polymerization, particularly in conjunction with thiol-ene chemistry. The two active radical species in a thiol-ene polymerization are the carbon-centered radical, which abstracts a hydrogen from a thiol group, and the

Scheme 1. Thiyl Radical Addition to and Subsequent Fragmentation of an Allyl Sulfide Functionality Demonstrating a Tris(methyl sulfide) Radical Intermediate and Rearrangement of Bonds, Where the Zigzag Lines Represent the Greater Polymer Network[a]

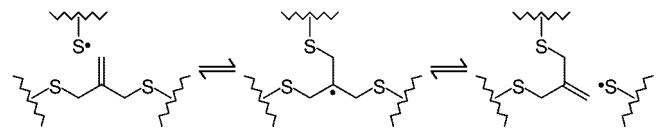

[a] Here the network topology is adaptable while maintaining invariant reactant and product concentrations and hence cross-link density.

* Corresponding author. E-mail: christopher.bowman@colorado.edu.
† Current address: Center for Bioengineering, Department of Mechanical Engineering, University of Colorado, Boulder, CO 80309-0427.

10.1021/ma802771b CCC: $40.75
Published on Web 03/10/2009

Scheme 2. Thiol-ene Polymerization Mechanism Where the Thiyl Radical Adds to a Vinyl Functional Group, Followed by Hydrogen Abstraction from a Thiol Functional Group Completing the Cycle and Forming a Carbon−Carbon Single Bond[a]

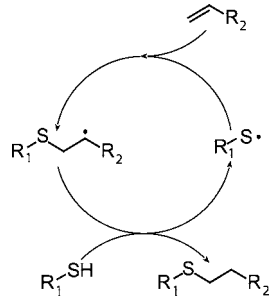

[a] In the ideal mechanism, chain transfer and addition steps alternate and proceed at the same overall rate.

sulfur-centered radical, which adds to a carbon−carbon double bond. Whereas the allyl sulfide moiety is a rather poor reversible addition−fragmentation chain transfer (RAFT) agent with respect to carbon-centered radicals,[19] it readily reacts with thiyl radicals generated within the thiol-ene polymerization chemistry.[26] Therefore, when the thiyl radical adds to the allyl sulfide carbon−carbon double bond, addition−fragmentation occurs, yielding a change in network topology without a net change in reactive species. (See Scheme 1.) Here we explore the effect of reversible allyl sulfide addition−fragmentation chain transfer during a thiol-ene photopolymerization on the evolution of polymerization-induced shrinkage stress. For comparison, an analogous propyl sulfide monomer, which is incapable of addition−fragmentation and the corresponding relaxation, was synthesized and polymerized under identical conditions. The resultant network should exhibit similar shrinkage, cross-link density, and homogeneity when compared to the allyl sulfide-containing material, allowing verification that stress relief is indeed coupled to the addition−fragmentation process and confirming the proposed stress relaxation mechanism.

Experimental Section

Characterization. Dynamic mechanical analysis (DMA) was performed in triplicate using a TA Instruments Q800 scanning at 1 °C/min from −80 to 100 °C at a frequency of 1 Hz and a strain of 0.1% in tension. The cross-link density was estimated from the elastic modulus, E', determined in the linear rubbery regime, which scales as the number of cross-links per volume in accordance with rubbery elasticity theory.[27] The glass-transition temperature (T_g) was assigned as the temperature at the tan δ curve maximum.

Polymerization conversion studies were performed on formulated resin sandwiched between two glass slides separated by 50 μm thick spacers and irradiated in situ using a high-pressure mercury vapor short arc lamp (EXFO Acticure 4000) equipped with a 365 nm narrow bandpass filter. Light intensity was measured using a radiometer equipped with a GaAsP detector (International Light IL1400A, model SEL005), a wide bandpass filter (model WBS320), and a quartz diffuser (model W). Conversions of thiol, vinyl ether, and allyl sulfide functional groups were determined by using infrared (IR) spectroscopy and monitoring the peak areas centered at 2570 cm^{-1} (PETMP thiol, S−H stretch), 3116 cm^{-1} (MDTVE and MeDTVE vinyl ether, C═C−H stretch), and 3077 cm^{-1} (MDTVE allyl, C═C−H stretch), respectively, using a Nicolet Magna-IR 750 series II FTIR spectrometer. Spectra at a resolution of 2 cm^{-1} were collected at a rate of five every 2 seconds. Deconvolution of the allyl and vinyl ether peaks for samples containing MDTVE was performed by subtracting the propyl sulfide-containing analogue spectrum from the allyl sulfide-containing spectrum, thus isolating the allyl absorption. All conversion

Scheme 3. Mercapto- and Vinyl-Based Monomers Used in This Study[a]

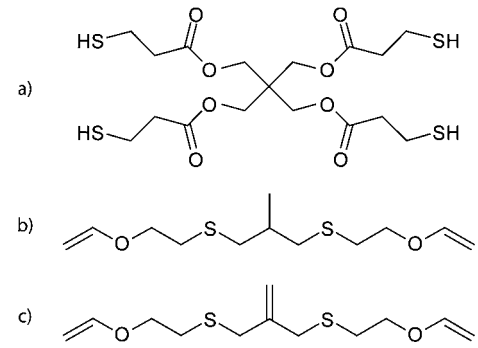

[a] (a) PETMP, (b) MeDTVE, and (c) MDTVE.

samples were formulated and measured in triplicate, and the presented data represent the mean of three runs where the standard errors were much smaller than the data points on the Figures.

Simultaneous polymerization stress and functional group conversion measurements were performed using a cantilever-type tensometer (American Dental Association Health Foundation) coupled to an IR spectrometer via optical fibers, as described in the literature.[28] Briefly, the resin was introduced into a 1 mm gap between two 6 mm diameter quartz rods, one of which was attached to an aluminum bar cantilever and the other to a solid base. The quartz rod ends were carefully cleaned and treated with 3-mercaptopropyltrimethoxysilane to ensure adhesion at the resin−quartz interface.[29] The sample was irradiated through one of the quartz rods, and we determined the tensile force developed by the sample shrinkage during polymerization by monitoring the aluminum bar deflection via a linear differential variable transformer (LDVT). Prior to the measurement, the deflection was calibrated using a force transducer. This calibration constant (i.e., the beam compliance) and the quartz rod area were used to convert the LDVT readings to stress measurements. Optical fibers were positioned to carry an IR signal to and from an IR spectrometer transverse through the sample. The vinyl ether conversion was determined by monitoring the peak area centered at 6185 cm^{-1} (C═C−H first overtone stretch) throughout the polymerization time; this peak was moderately overlapped by the allyl sulfide peak but was readily deconvoluted using Gaussian fitting. All polymerizations were performed at ambient temperature.

Materials. 3-Mercaptopropyltrimethoxysilane was purchased from Gelest. 3-Chloro-2-chloromethyl-1-propene (96%), potassium ethyl xanthogenate (97%), 2-chloroethyl vinyl ether (95%), sodium bromide (>99%), ethylenediamine (>98%), and sulfuric acid (98%) were purchased from Fisher Scientific. 2-Methyl-1,3-propanediol (99%) and sodium metal (99%) were purchased from Sigma-Aldrich. Pentaerythritol tetra(3-mercaptopropionate) (PETMP, shown in Scheme 3a) and Irgacure 184 (1-hydroxy-cyclohexyl-phenyl-ketone) were obtained from Evans Chemetics and Ciba Specialty Chemicals, respectively, and were used without further purification.

Synthesis of 2-Methylpropane-1,3-di(thioethyl vinyl ether) (MeDTVE, Scheme 3b). 2-Methyl-1,3-dibromopropane was synthesized following a modified procedure from literature,[30] and the synthesis of 2-methyl-1,3-dimercaptopropane and subsequent synthesis of 2-methylpropane-1,3-di(thioethyl vinyl ether) followed the procedure found in refs 31 and 32. Synthesis of these compounds is summarized below.

Synthesis of 2-Methyl-1,3-dibromopropane. Sodium bromide (258 g, 2.5 mol) was added to 225 mL of water in a 2 L round-bottomed flask equipped with a reflux condenser with stirring. 2-Methyl-1,3-propanediol (90.12 g, 1 mol) was then added, followed by the gradual addition of 226 mL (4.25 mol) of sulfuric acid. The solution was heated to reflux for 2 h, and the product was subsequently obtained by distillation from the reaction mixture. The product was washed with an aqueous 2 M sulfuric acid solution and then with

Table 1. DMA Measurements for a 1:1 Vinyl Ether/Thiol Stoichiometric Ratio of MDTVE/PETMP or MeDTVE/PETMP Formulated with 0.5 wt % Irgacure 184 and Irradiated at 30 mW/cm^2 of 365 nm Light for 5 min

	glassy modulus	rubbery modulus	
material	$E'(T = -50\ °C)$	$E'(T = 20\ °C)$	T_g − max(tan δ)
MeDTVE/PETMP	1.7 ± 0.2 GPa	10.8 ± 0.2 MPa	−26.6 ± 0.3 °C
MDTVE/PETMP	1.8 ± 0.1 GPa	12.2 ± 0.1 MPa	−19 ± 1 °C

an aqueous 10 wt % sodium carbonate solution. The product was then dried over calcium chloride and purified by distillation to give 155 g (72%) of a dense, clear liquid that became increasingly purple over time. ^{1}H NMR (500 MHz, $CDCl_3$, δ): 3.49 (ddd, J = 5.5, 10.1, 16.2, 4H), 2.24−2.13 (m, 1H), 1.15 (d, J = 6.7, 3H).

Synthesis of 2-Methyl-1,3-dimercaptopropane. Potassium ethyl xanthogenate (125 g, 778 mmol) was added to 125 mL of absolute ethanol and purged with argon. A 50% v/v solution of 80 g (371 mmol) of freshly distilled 2-methyl-1,3-dibromopropane in ethanol was added dropwise to the potassium ethyl xanthogenate−ethanol suspension, and the solution was stirred overnight. The product was obtained using liquid−liquid water−ether extraction. The etheric solution was dried over calcium chloride, and the ether evaporated to give 103 g of a crude, light-yellow oil. ^{1}H NMR (500 MHz, $CDCl_3$, δ): 4.64 (q, J = 7.1, 4H), 3.18 (ddd, J = 6.6, 13.7, 20.8, 4H), 2.31−2.21 (m, 1H), 1.42 (t, J = 7.1, 6H), 1.12 (d, J = 6.8, 3H). This crude yellow oil was added dropwise to 200 mL of ethylenediamine in an ice bath and, upon complete addition, was allowed to react no longer than 2 h. Finally, this mixture was then acidified by cautious addition to a flask of sulfuric acid (500 mL) and ice, yielding a malodorous mixture. The product was obtained using liquid−liquid water−ether extraction. The etheric solution was dried over calcium chloride, and the ether evaporated. The residual oil was then vacuum distilled to give 24.0 g (53%) of a slightly yellow oil. ^{1}H NMR (500 MHz, $CDCl_3$, δ): 2.67−2.54 (m, 4H), 1.86−1.75 (m, 1H), 1.26 (t, J = 8.4, 2H), 1.04 (d, J = 6.7, 3H).

Synthesis of 2-Methylpropane-1,3-di(thioethyl vinyl ether). A 50% v/v solution of 24 g (196 mmol) of 2-methyl-1,3-dimercaptopropane and 44 g (413 mmol) of chloroethyl vinyl ether in methanol was prepared and added to a refluxing solution of sodium in methanol under argon protection. The reaction was allowed to react for 2 h, and it was then purified using liquid−liquid water−ether solution and dried over calcium chloride. The ether evaporated, and the product was vacuum distilled to give 40.2 g (78%) of clear oil. ^{1}H NMR (500 MHz, $CDCl_3$, δ): 6.46 (dd, J = 6.8, 14.4, 2H), 4.19 (dd, J = 2.2, 14.3, 2H), 4.03 (dd, J = 2.2, 6.8, 2H), 3.85 (t, J = 6.7, 4H), 2.77 (t, J = 6.7, 4H), 2.62 (ddd, J = 6.5, 12.8, 92.4, 4H), 2.00−1.86 (m, 1H). 1.09 (d, J = 6.7, 3H).

2-Methylene-propane-1,3-di(thioethyl vinyl ether) (MDTVE, Scheme 3c). The synthesis of MDTVE was previously described in the literature[31] and is analogous to the procedure described above for MeDTVE, where the commercially available 3-chloro-2-chloromethyl-1-propene replaces 2-methyl-1,3-dibromopropane. ^{1}H NMR (500 MHz, $CDCl_3$, δ): 6.45 (dd, J = 6.8, 14.3, 2H), 5.04 (s, 2H), 4.19 (dd, J = 2.2, 14.3, 2H), 4.03 (dd, J = 2.2, 6.8, 2H), 3.83 (t, J = 6.7, 4H), 3.35 (s, 4H), 2.69 (t, J = 6.7, 4H).

Results and Discussion

The allyl sulfide divinyl ether monomer (MDTVE) and its propyl sulfide divinyl ether analogue (MeDTVE) were photopolymerized with PETMP in a 1:1 vinyl ether/thiol stoichiometric ratio. The two divinyl ether monomers have nearly identical chemical structures and molecular weights, where the central carbon is either a planar sp^2 or tetrahedral sp^3 configuration in the MDTVE or MeDTVE monomers, respectively. (See Scheme 3.) The cured polymeric networks exhibit similar thermomechanical properties, as shown in Table 1, which is indicative of similar network structures. Nevertheless, the material incorporating the allyl sulfide functionality has a larger elastic modulus and a higher T_g, suggesting that the network has a slightly higher cross-link density, a less flexible backbone, or both.

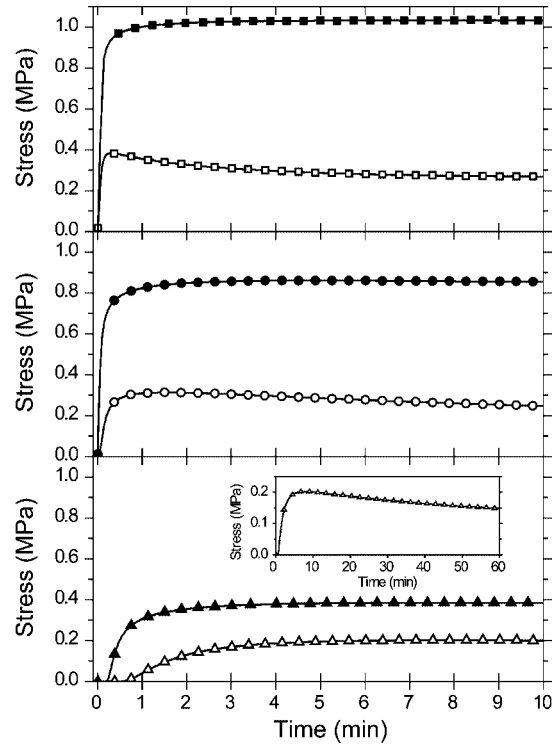

Figure 1. Polymerization stress for a 1:1 vinyl ether/thiol stoichiometric ratio of MeDTVE/PETMP (filled symbols) and MDTVE/PETMP (open symbols) irradiated at 10.0 (top panel, squares), 1.0 (middle panel, circles), and 0.1 (bottom panel, triangles) mW/cm^2. The inset in the bottom panel is MDTVE/PETMP irradiated at 0.1 mW/cm^2 for 60 min. All samples were formulated with 0.8 wt % Irgacure 184 and irradiated with 365 nm light. For clarity, not all data points are shown.

In Figure 1, the shrinkage stress evolution during the photopolymerization of allyl sulfide-based MDTVE/PETMP (open symbols) and propyl sulfide-based MeDTVE/PETMP (filled symbols) thiol-ene resins at three intensities is shown. Despite possessing a slightly higher rubbery modulus and cross-link density (Table 1), the allyl sulfide-containing material has a dramatically reduced polymerization-induced shrinkage stress. The allyl sulfide-containing material exhibits as little as one-fourth of the volume-induced shrinkages stress as compared with that of the material containing the propyl sulfide analogue. Moreover, the stress evolution of the allyl sulfide-containing material demonstrates a maximum, followed by a gradual, continuous stress relaxation. As illustrated in the three panels of Figure 1, both the stress development rate and the ultimate stress decrease with reduced irradiation intensity. The final stress is the superposition of stored and dissipated stress as the material contracts; this complex viscoelastic behavior is compounded as the material is structurally evolving throughout the polymerization. At sufficiently high polymerization rates, and hence deformation rates (i.e., large polymerization-induced volume shrinkage rates), the material possesses solidlike character, storing stress prior to gelation and yielding a higher accumulated or final stress. Conversely, pregelation shrinkage stress is dissipated via flow at low polymerization rates, reducing the final stress.

The conversion of vinyl ether and thiol for MDTVE/PETMP and MeDTVE/PETMP photopolymerized at the same irradiation intensity is shown in Figure 2. The polymerization rate is slower for the allyl sulfide-containing material because the allyl sulfide functionality and the vinyl ether compete in reactions with the thiyl radical. The allyl sulfide functionality acts as a chain

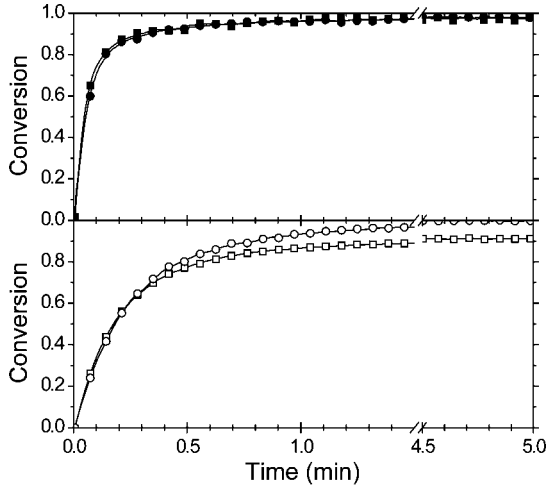

Figure 2. Conversion of vinyl ether (square) and thiol (circle) functional groups for a 1:1 vinyl ether/thiol stoichiometric ratio of MeDTVE/PETMP (top panel, filled symbols) and MDTVE/PETMP (bottom panel, open symbols) for thin-film samples irradiated at 10 mW/cm^2 of 365 nm light. For clarity, not all data points are shown.

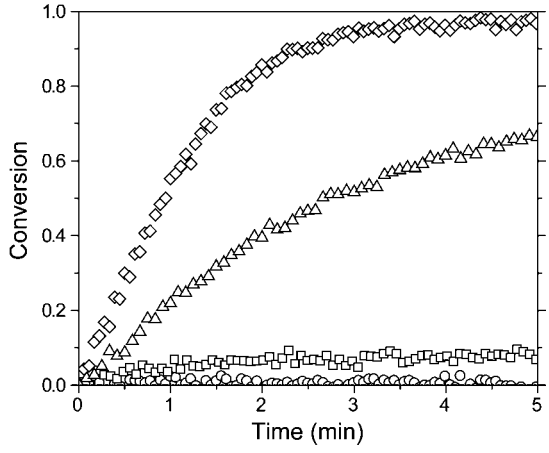

Figure 3. Conversion of allyl sulfide functional groups in a 5:3 (○), 1:1 (□), 3:5 (△), and 1:3 (◇) vinyl ether/thiol stoichiometric ratio of functional groups for a MDTVE/PETMP polymerization. Thin-film samples were irradiated at 10 mW/cm^2 of 365 nm light. For clarity, not all data points are shown.

transfer agent, which, upon reaction with a thiyl radical, temporarily sequesters the radical and reduces the polymerization rate. As the polymerization proceeds, the vinyl ether functionality is consumed, thus increasing the likelihood of thiyl radicals reacting with the relatively more abundant allyl sulfide functionality. Interestingly, unlike the thiol functional group (Figure 2b), the vinyl ether functional group in the MDTVE/PETMP sample does not reach full conversion, suggesting thiol consumption by an alternate mechanism that is not indicated in Schemes 1 or 2.

There has been significant debate within the literature on whether intramolecular homolytic substitution of the allyl sulfide (S_H2', i.e., addition−fragmentation) occurs via a concerted or stepwise mechanism.[15,18,33,34] For a concerted addition−fragmentation mechanism, the tris(methyl sulfide) radical intermediate (shown in Scheme 1) would not exist, prohibiting potential side reactions and thus conserving the allyl sulfide concentration throughout the polymerization; however, as shown in Figure 3, consumption of allyl sulfide is observed. Indeed, increasing the stoichiometric imbalance in favor of excess thiol results in increased allyl sulfide consumption, which is inconsistent with a concerted mechanism. Alternatively, the existence of a

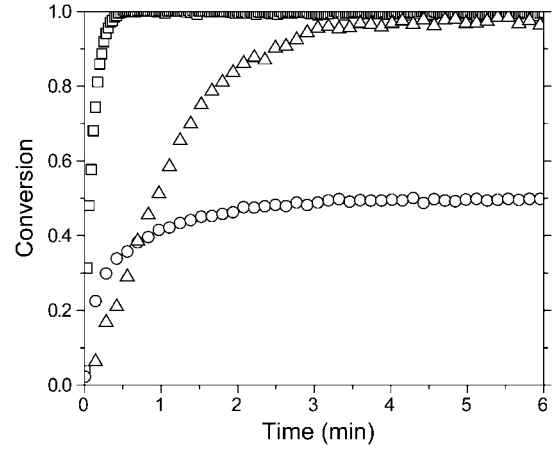

Figure 4. Conversion of vinyl ether (□), thiol (○), and allyl sulfide (△) functional groups versus polymerization time for a 1:3 vinyl ether/thiol functional group stoichiometric ratio of MDTVE/PETMP. Thin-film samples were irradiated at 10 mW/cm^2 of 365 nm light. For clarity, not all data points are shown.

Scheme 4. Proposed Thiol-ene/Allyl Sulfide Reaction Mechanism Where the Thiyl Radical May Participate in Either the Thiol-ene Polymerization (Left Cycle) or Allyl Sulfide Addition−Fragmentation (Right Cycle)[a]

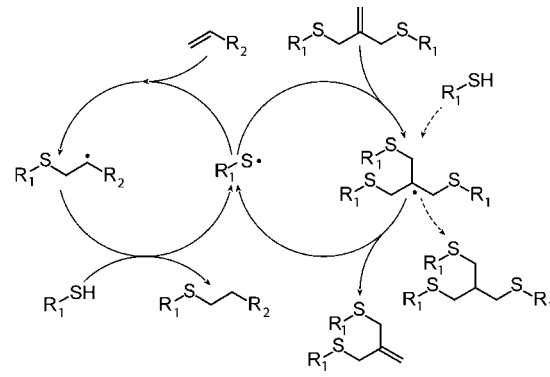

[a] Hydrogen abstraction from thiol by the tris(methyl sulfide) radical is indicated by the dashed line.

tris(methyl sulfide) radical intermediate would enable hydrogen abstraction from a thiol group, which is consistent with a stepwise mechanism. This side reaction is further established by simultaneously monitoring thiol, vinyl ether, and allyl sulfide functional group conversions, revealing that the thiol functional group reacts well after the vinyl functionality is completely consumed, as shown in Figure 4. The excess thiol formulation, containing a 1:3 vinyl ether/thiol stoichiometric mixture of MDTVE to PETMP (1:2 total vinyl/thiol), demonstrates that the allyl sulfide and vinyl ether functional groups approach complete conversion while the thiol functional group approaches 50% conversion; this equates to a 1:1 reaction between thiol and all carbon−carbon double bonds. The presence of this side reaction with thiol is attributable to allyl sulfide addition−fragmentation proceeding via a stepwise mechanism.

The simultaneous thiol-ene/allyl sulfide reaction mechanism is proposed in Scheme 4, which incorporates addition−fragmentation into the thiol-ene polymerization mechanism. When the thiyl radical is formed, it undergoes radical-mediated addition to either vinyl ether or allyl sulfide. Upon reaction with allyl sulfide, the tris(methyl sulfide) radical intermediate either fragments, regenerating allyl sulfide and thiyl radical, or abstracts a hydrogen atom from a thiol; this side reaction can be considered to be akin to the thiol-ene polymerization of thiols with allyl sulfides. The thiol-ene polymerization mechanism,

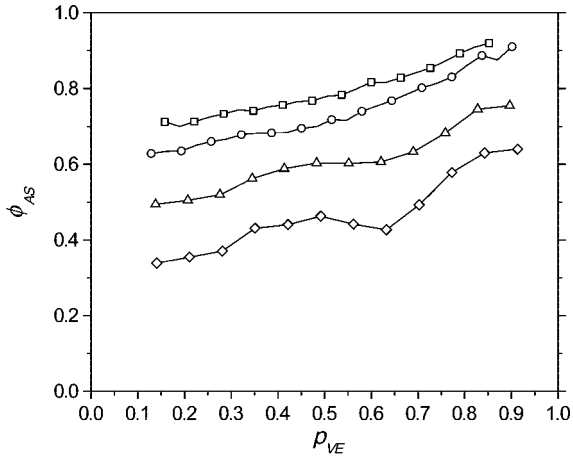

Figure 5. Thiyl radical mole fraction in the allyl sulfide cycle (ϕ_{AS}) versus the vinyl ether conversion (p_{VE}) for a 100:0 (□), 75:25 (○), 50:50 (△), and 25:75 (◇) MDTVE/MeDTVE mixture formulated with a 1:1 vinyl ether/thiol stoichiometric balance with PETMP.

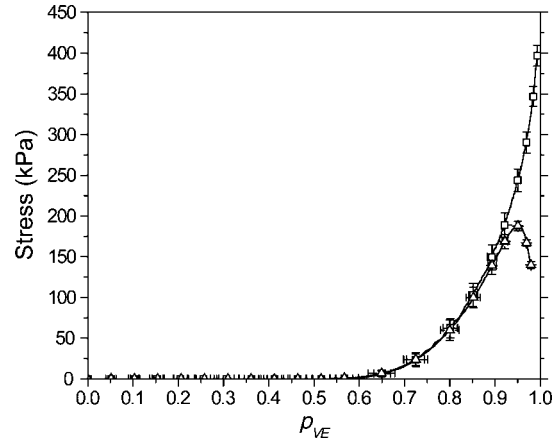

Figure 6. Stress versus vinyl ether conversion (p_{VE}) for a 1:1 vinyl ether/thiol stoichiometric ratio of MeDTVE/PETMP (□) and MDTVE/PETMP (△) irradiated at 0.1 mW/cm^2 of 365 nm for 60 min. For clarity, not all data points are shown.

regardless of whether it occurs in the vinyl ether or allyl sulfide cycle, results in the loss of a thiol and the concomitant creation of a thioether. Therefore, networks that have similar thiol conversion should have similar cross-link densities, as observed in the DMA (Table 1).

As described previously, the observed reduction in the vinyl ether consumption rate is attributed to the allyl sulfide functionality temporarily sequestering a fraction of the thiyl radical concentration. A vinyl ether species balance allows the thiyl radical concentration, [S•], to be expressed in terms of k_p, the reaction rate constant for propagation of the thiyl radical through the vinyl ether, and vinyl ether conversion, p_{VE}, as

$$[\mathrm{S}\bullet] = -\frac{1}{k_p[\mathrm{VE}]}\frac{\mathrm{d}[\mathrm{VE}]}{\mathrm{d}t} = \frac{1}{k_p(1-p_{VE})}\frac{\mathrm{d}p_{VE}}{\mathrm{d}t}$$

where [VE] is the vinyl ether concentration. A comparison of the vinyl ether consumption rate in the propyl and allyl sulfide-containing polymerizations reveals the fraction of thiyl radicals sequestered by the allyl sulfide, ϕ_{AS}, to be

$$\phi_{AS} \equiv 1 - \frac{[\mathrm{S}\bullet]_{MDTVE}}{[\mathrm{S}\bullet]_{MeDTVE}} = 1 - \left.\frac{\mathrm{d}p_{VE,MDTVE}}{\mathrm{d}p_{VE,MeDTVE}}\right|_{p_{VE,MDTVE}=p_{VE,MeDTVE}}$$

Here k_p is assumed to be equivalent for MDTVE and MeDTVE because the difference in the functionality incorporated in the backbone of these monomers should have a minimal impact on the terminal vinyl ether functionalities. The instantaneous rates of conversion for allyl and propyl sulfide-based resins were evaluated at equivalent conversions, demonstrating that the allyl sulfide cycle sequesters >70% of the available thiyl radicals shortly after the polymerization begins (squares, Figure 5). The allyl sulfide concentration effect was evaluated by mixing MDTVE and MeDTVE in various ratios, allowing the independent manipulation of the ratio of allyl sulfide to vinyl ether while holding the vinyl ether-to-thiol ratio constant. The competition between the two vinyl groups to react with the thiyl radical is demonstrated in Figure 5, where the thiyl radical sequestration increases with increasing allyl sulfide concentration and, as the polymerization proceeds, with decreasing vinyl ether concentration. This behavior is consistent with the proposed reaction mechanism shown in Scheme 4.

Shrinkage stress as a function of vinyl ether conversion, obtained by coupling simultaneous tensometry and IR spectroscopy, is shown in Figure 6. These photopolymerizations were performed using low light intensity (0.1 mW/cm^2 at 365 nm), reducing the polymerization rate, and minimizing the possibility of accumulated stress in the pregel regime. The gel-point conversion, predicted by the Flory−Stockmayer equation[35,36] to be 0.58, closely coincides with the location of the polymerization stress initiation. The postgelation stress evolution for the allyl sulfide-containing material is markedly different from the propyl sulfide-containing material, which is attributed to addition−fragmentation chain transfer through the network backbone that dominates the latter stages of the polymerization. (See Figure 5.) Aside from the significantly reduced final stress, there is an apparent maximum and subsequent relaxation in the stress evolution. The decrease in stress occurring beyond 92% vinyl ether conversion relates to stress relaxation that is occurring after the thiol functionality is completely consumed. (See Figure 2.) This postpolymerization stress relaxation is characteristic of allyl sulfide addition−fragmentation, as observed in previous postpolymerization studies of similar materials.[14] In the absence of thiol, the carbon-centered radical generated by the propagation of a thiyl radical through a vinyl ether (see the thiol-ene polymerization cycle, Scheme 4) is incapable of undergoing subsequent propagation or chain transfer events. Therefore, in this regime, these carbon-centered radicals exclusively participate in termination events, reducing the proportion of radicals available for addition−fragmentation chain transfer.

Conclusions

Allyl sulfide addition−fragmentation in a radical-mediated thiol-ene polymerization reduces polymerization-induced shrinkage stress. Comparison of the photopolymerizations of allyl sulfide- and propyl containing thiol-ene materials allowed the effect of addition−fragmentation on polymerization rate and shrinkage stress evolution to be isolated. The allyl sulfide functionality acts as an addition−fragmentation chain transfer agent, sequestering radical species and reducing the polymerization rate. Moreover, the addition−fragmentation mechanism provides a pathway for network rearrangement and significantly reduces polymerization stress. It was further shown that addition−fragmentation proceeds via a stepwise mechanism, allowing for an irreversible side reaction whereby the radical intermediate abstracts hydrogen from thiol. This side reaction reduces both the allyl sulfide functional group concentration and the proportion of radicals available for addition−fragmentation chain transfer due to residual, unreacted vinyl ether. Consequently, this side reaction leads to inhibition of the stress

relaxation mechanism. Nevertheless, thiyl radical addition to allyl sulfide predominantly results in addition−fragmentation and is an effective pathway for reducing polymerization-induced shrinkage stress. Indeed, addition−fragmentation chain transfer provides a novel avenue for future stress reduction strategies applied to other network-forming polymerizations.

Acknowledgment. We acknowledge funding from the National Institutes of Health, NIH grant DE10959.

References and Notes

(1) Bowman, C. N.; Kloxin, C. J. *AIChE J.* **2008**, *54*, 2775.
(2) Jacobine, A. F. In *Radiation Curing in Polymer Science and Technology*; Fouassier, J. P., Rabek, J. F., Eds.; Elsevier Applied Science: London, 1993; Vol. III, pp 219−268.
(3) Woods, J. G. In *Radiation Curing: Science and Technology*; Pappas, S. P., Ed.; Plenum Press: New York, 1992.
(4) Kloosterboer, J. G. *Adv. Polym. Sci.* **1988**, *84*, 1.
(5) Zwiers, R. J. M.; Dortant, G. C. M. *Appl. Opt.* **1985**, *24*, 4483.
(6) Lovell, L. G.; Berchtold, K. A.; Elliott, J. E.; Lu, H.; Bowman, C. N. *Polym. Adv. Technol.* **2001**, *12*, 335.
(7) Lu, H.; Carioscia, J. A.; Stansbury, J. W.; Bowman, C. N. *Dent. Mater.* **2005**, *21*, 1129.
(8) Stansbury, J. W.; Bowman, C. N.; Newman, S. M. *Phys. Today* **2008**, *61*, 82.
(9) Carioscia, J. A.; Lu, H.; Stanbury, J. W.; Bowman, C. N. *Dent. Mater.* **2005**, *21*, 1129.
(10) Tilbrook, D. A.; Clarke, R. L.; Howle, N. E.; Braden, M. *Biomaterials* **2000**, *21*, 1743.
(11) Stansbury, J. W. *J. Dent. Res.* **1992**, *71*, 1408.
(12) Bucknall, C. B.; Davies, P.; Partridge, I. K. *Polymer* **1985**, *26*, 109.
(13) Inoue, T. *Prog. Polym. Sci.* **1995**, *20*, 119.
(14) Scott, T. F.; Schneider, A. D.; Cook, W. D.; Bowman, C. N. *Science* **2005**, *308*, 1615.
(15) Hall, D. N.; Oswald, A. A.; Griesbaum, K. *J. Org. Chem.* **1965**, *30*, 3829.
(16) Hall, D. N. *J. Org. Chem.* **1967**, *32*, 2082.
(17) Migita, T.; Kosugi, M.; Takayama, K.; Nakagawa, Y. *Tetrahedron* **1973**, *29*, 51.
(18) Barton, D. H. R.; Crich, D. *J. Chem. Soc., Perkin Trans. 1* **1986**, 1613.
(19) Meijs, G. F.; Rizzardo, E.; Thang, S. H. *Macromolecules* **1988**, *21*, 3122.
(20) Evans, R. A.; Moad, G.; Rizzardo, E.; Thang, S. H. *Macromolecules* **1994**, *27*, 7935.
(21) Evans, R. A.; Rizzardo, E. *Macromolecules* **1996**, *29*, 6983.
(22) Morgan, C. R.; Magnotta, F.; Ketley, A. D. *J. Polym. Sci., Polym. Chem. Ed.* **1977**, *15*, 627.
(23) Hoyle, C. E.; Lee, T. Y.; Roper, T. *J. Polym. Sci., Part A: Polym. Chem.* **2004**, *42*, 5301.
(24) Walling, C. *J. Am. Chem. Soc.* **1945**, *67*, 441.
(25) Reddy, S. K.; Okay, O.; Bowman, C. N. *Macromolecules* **2006**, *39*, 8832.
(26) Cook, W. D.; Chausson, S.; Chen, F.; Le Pluart, L.; Bowman, C. N.; Scott, T. F. *Polym. Int.* **2008**, *57*, 469.
(27) Flory, P. J. *Principles of Polymer Chemistry*; Cornell University Press: Ithaca, NY, 1953.
(28) Lu, H.; Stansbury, J. W.; Dickens, S. H.; Eichmiller, F. C.; Bowman, C. N. *J. Mater. Sci.: Mater. Med.* **2004**, *15*, 1097.
(29) Walba, D. M.; Liberko, C. A.; Körblova, E.; Farrow, M.; Furtak, T. E.; Chow, B. C.; Schwartz, D. K.; Freeman, A. S.; Douglas, K.; Williams, S. D.; Klittnick, A. F.; Clark, N. A. *Liq. Cryst.* **2004**, *31*, 481.
(30) Kamm, O.; Marvel, C. S. *Org. Synth.* **1921**, *1*, 1.
(31) Scott, T. F.; Draughon, R. B.; Bowman, C. N. *Adv. Mater.* **2006**, *18*, 2128.
(32) Evans, R. A.; Rizzardo, E. *J. Polym. Sci., Part A: Polym. Chem.* **2001**, *39*, 202.
(33) Griesbaum, K. *Angew. Chem., Int. Ed. Engl.* **1970**, *9*, 273.
(34) Wu, Y. W.; Huang, H. T.; Chen, Y.; Yang, J. F. *Tetrahedron* **2006**, *62*, 6061.
(35) Flory, P. J. *J. Am. Chem. Soc.* **1941**, *63*, 3083.
(36) Stockmayer, W. H. *J. Chem. Phys.* **1943**, *11*, 45.

MA802771B